Journal of Engineering and Sustainable Development
www.jeasd.org
Vol. 22, No.01, January 2018
ISSN 2520-0917

# OPTIMAL CONTROLLER FOR VECTOR-CONTROLLED MULTILEVEL INVERETER FED BRUSHLESS DC MOTOR

Dr. Turki Kahyoosh Hassan [1], Mustafa Bashar Abdulmelik[2*]

1) Asst. Prof., Electrical Engineering Department, Al-Mustansiriyah University, Baghdad, Iraq.
2) M.Sc. Student., Electrical Engineering Department, Al-Mustansiriyah University, Baghdad, Iraq.

**Abstract:** This paper presents a high performance brushless DC (BLDC) motor drive system that achieves optimal speed response with minimized torque ripple and low total harmonic distortion (THD). The speed controller is optimally tuned using particle swarm optimization (PSO) technique; and the torque ripple is minimized by using vector control instead of the six-step (trapezoidal control) and by using multilevel inverter to lower the THD of the voltages and currents. The proposed system alongside the traditional six-step technique, are modeled and simulated in MATLAB/Simulink program; and their simulation results are compared and discussed. The obtained results show that the proposed system speed response and torque ripple are greatly improved compared with the six-step technique.

**Keywords**: *Particle Swarm Optimization, Speed Controller, Vector Control, BLDC Motor, Multilevel Inverter.*

## مسيطر مثالي لمحرك التيار المستمر عديم الفرش المسيطر اتجاهياً و المغذى بمبدل متعدد المستويات

**الخلاصة:** هذه الوثيقة تقدم نظام مسوق عالي الاداء لمحرك التيار المستمر عديم الفرش الذي يحقق استجابة سرعة مثالية مع ذبذبة عزم مصغرة و مجموع تشوه توافقي قليل. مسيطر السرعة منغم مثالياً بأستخدام طريقة تحسين سرب الجسميات؛ و تذبذب العزم مصغر بأستخدام المسيطر الأتجهاي بدلاً من سيطرة الست-خطوات (الشبه منحرف) و بأستخدام مبدل متعدد المستويات لتقليل مجموع التشوه التوافقي للفولتيات و التيارات. النظام المقترح أضافة الى الطريقة التقليدية, مركبة و محاكاة في برنامج ماتلاب/سيميولنك؛ و تمت مقارنة و مناقشة نتائج محاكاتهم. النتائج التي تم الحصول عليها تبين أن اداء السرعة و تذبذب العزم للناظام المقترح تحسن بصورة كبيرة مقارنة بطريقة الست-خطوات.

## 1. Introduction

Permanent magnet (PM) motors have been rapidly increasing in popularity in the recent years due to their high efficiency and low power density compared with the wound type motors. PMM motors are generally classified into two types: the permanent magnet synchronous motor (PMSM) and the BLDC motor. These motors are basically the same except for the different shapes of their back electromotive force (BEMF), which is sinusoidal in case of PMSM and trapezoidal in case of BLDC motor [1].

BLDC motor is simpler and less expensive than PMSM; however, the latter has a higher torque ripple, which is mostly due to the high distortion in the current waveform

*CorrespondingAuthor mustafa.b_alqaseer@yahoo.com

associated with the six-step or trapezoidal control. Torque ripple causes vibration and shortens the life span of the motor and therefore it should be minimized. Many attempts were made to reduce the torque ripple of BLDC motor.

Lee *et al.* [2] proposed a method to reduce the torque ripple by varying the pulse-width modulation (PWM) duty ratio of the non-commutated phase to remove voltage disturbance during current commutation. However, this method requires precise computations to synchronize the PWM signal with the end of the commutation.

On the other hand, Wang [3] found that the torque ripple can be reduced by 50% compared with the traditional technique by using a modified sinusoidal pulse-width modulation (SPWM). However, this method requires current control loop to achieve faster dynamic response.

Doss *et al.* [4] proposed using cascaded H-bridge multilevel inverter with current controller to reduce torque ripple and lower the THD of the currents. This method obtained good results of reducing the torque ripple and lowering the THD of the currents; however, the speed and torque performance at low speeds was not addressed, which is an issue in trapezoidal control.

Proportional-integral-derivative (PID) and proportional-integral (PI) controllers are probably the most popular controllers that are used in speed and current control due to their simple three/two term functionality that provides robust performance in transient and steady-states [5]. The tuning of these controllers however can be a difficult task with systems having different degrees of nonlinearities and varying parameters such as the resistance and moment of inertia of the motor.

Yu and Hwang [6] found that by using a linear-quadratic regulator (LQR), the optimal parameters for the PID controller could be obtained. The obtained response was near optimal; however, this method is very reliant on the system parameters.

Rubaai *et al.* [7] presented a hybrid fuzzy PID controller for speed control of BLDC motors; the method was found to have superior performance compared with the conventional PID controllers regarding external disturbances and nonlinearities.

Kandiban and Arulmozhiyal [8] proposed an adaptive fuzzy PID controller to control the speed of BLDC motor. The experimental results showed that the adaptive fuzzy PID controller has better control performance than the fuzzy PID controllers and conventional PID controllers.

Ravi *et al.* [9] proposed genetic algorithm method to optimize the PID gains for the control of BLDC motor. The proposed controller was found efficient and yielded faster response than the conventional controllers were. However, detailed information for the dynamics of the speed and torque responses was not presented.

Rathika and Ravichandran [10] proposed using PSO method to find the optimal PID speed controller gains for BLDC motor. This method was shown to improve dynamic speed performance over the conventional tuning methods.

In this paper, an optimal speed controller for BLDC motor is attained using PSO technique; and the torque ripple is reduced by using vector control and by lowering the THD of the voltages and currents using multilevel inverter. The paper contribution is obtaining a BLDC motor drive system that achieves optimal speed response and minimized the torque ripple.

The paper is organized as follows: sections 2, 3 and 4 gives a brief overview of BLDC motor, vector control and multilevel inverter respectively, section 5 describes the Particle Swarm Optimization method and fitness function assignment and calculation, section 6 describes the proposed system, section 7 presents and discusses the obtained results, section 8 gives the conclusions and possible future work and section 9 contains the references.

## 2. BLDC Motor

BLDC motor is a type of synchronous motors; it consists of a stator that contains windings; and a rotor that contains permanent magnets. This motor has many advantages over the conventional DC motor such as higher efficiency, little maintenance, high power density and low volume.

The operation of the motor in six-step control is done by switching ON two phases at a time according to the rotor position so that the generated electromagnetic field drags the rotor with it by the force of attraction. The switched ON phases changes on every 60 degrees making a total of six switching states in one cycle. The modelling for BLDC motor is similar to the brushed DC motor, which is shown in the following equations [11, 12]:

$$\begin{bmatrix} v_a \\ v_b \\ v_c \end{bmatrix} = \begin{bmatrix} R_s & 0 & 0 \\ 0 & R_s & 0 \\ 0 & 0 & R_s \end{bmatrix} \begin{bmatrix} i_a \\ i_b \\ i_c \end{bmatrix} + \begin{bmatrix} L_s & 0 & 0 \\ 0 & L_s & 0 \\ 0 & 0 & L_s \end{bmatrix} \frac{d}{dt} \begin{bmatrix} i_a \\ i_b \\ i_c \end{bmatrix} + \begin{bmatrix} e_a \\ e_b \\ e_c \end{bmatrix} \quad (1)$$

where $v_a$, $v_b$ and $v_c$ are the phase voltages ; $i_a$, $i_b$ and $i_c$ are the stator currents, $e_a$, $e_b$ and $e_c$ are the BEMFs, $R_s$ is the stator winding resistance and $L_s$ is the stator winding inductance. The generated torque by the motor is found by the following equation:

$$T_e = \frac{e_a i_a + e_b i_b + e_c i_c}{\omega_m} \quad (2)$$

where $\omega_m$ is the mechanical rotor speed of the motor. The dynamic equation for the motor is given by:

$$T_{e-}T_L = J\frac{d\omega_m}{dt} + B\omega_m \quad (3)$$

where $T_L$ is the load torque, $J$ is the moment of inertia of the system and $B$ is the friction coefficient.

The BLDC motor specifications used in this paper are listed in the following table [13]:

Table 1. Motor Specifications

| Rated voltage | 500 V |
|---|---|
| Rated speed | 3000 rpm |
| Rated torque | 3 N.m |
| Rated power | 1 kW |
| Stator resistance | 2.875 Ω |
| Stator inductance | 8.5e-3 H |
| Voltage constant ($K_e$) | 146.6077 v/krpm |
| Torque constant ($K_t$) | 1.4 N.m/A |
| Flux linkage | 0.175 wb |
| Number of pole pairs (P) | 4 |

## 3. Vector Control

Vector or field-oriented control is a type of control technique that transforms the stator currents from three-phase system in the stationary frame (a-b-c coordinates), into two orthogonal DC components in the rotating reference frame (d-q coordinates). The d-axis current is the flux component; and the q-axis current is the torque component. Therefore, the flux and the torque are controlled independently similar to a DC motor resulting in a number of advantages such as faster dynamic response, improved transient and steady state performance and higher efficiency [14, 15].

## 4. Multilevel Inverters

In recent years, multilevel inverters have been widely spreading in industry especially in high power medium voltage drives due to their ability of achieving high power ratings and producing a voltage waveform with low THD. These devices synthesize the output voltage to form staircase shaped waveform consisting of multiple levels of voltages. Multilevel inverters have several advantages over the two-level inverters aside from lowering the distortion in the output voltages. These advantages summarized as follows: reduction of the dv/dt stress on the power switches, low common mode (CM) voltage which reduces the stress on the bearings of the motor fed by the inverter, low distortion in the input current and their ability to operate at fundamental as well as high switching frequencies [16, 17].

Multilevel inverters have three main topologies: the diode-clamped, flying capacitors and cascaded H-bridges topologies. The diode-clamped inverter has a problem of voltage unbalance and requires a large number of semiconductor devices; while the flying capacitors inverter requires a large number of capacitors that are quite expensive and bulky. The CHB inverter have the least problems compared with the other topologies but requires independent DC voltage sources.

There are several modulation techniques for multilevel inverters; the most common technique is the sinusoidal pulse width modulation (SPWM). This technique consists of a number of carrier signals equal to (n-1) where n is the number of levels. These carrier signals are compared with the modulating signals to give the SPWM signals. The SPWM technique is divided into two main types: phase-shifted SPWM and level-shifted SPWM [18]. In this paper, the CHB topology and the level shifted-shifted SPWM modulation are considered.

## 5. Particle Swarm Optimization (PSO)

PSO is an optimization method that is based on the flocking of birds or the schooling of fish where the individuals or particles have a tendency of changing their positions to a position best suitable for food. It was first developed in 1995 by Kennedy and Eberhart [19, 20]. To obtain optimal speed response, this optimization method is applied to the PID controller of the speed to find the optimal parameters of the controller ($K_p$, $K_i$ and $K_d$). PSO method starts by generating random positions for the particles in a defined search space; then, each particle is assigned with a fitness value that signifies how close the particle is from the solution. The velocities of the particles are then calculated for the following equation:

$$v_i(k+1) = w.v_i(\mathrm{k}) + c_1 r_1(\mathrm{k})\left(p_{best,i}(\mathrm{k}) - x_i(\mathrm{k})\right) + c_2 r_2(\mathrm{k})\left(g_{best}(\mathrm{k}) - x_i(\mathrm{k})\right) \tag{4}$$

where w is the inertia weight, $v_i(k+1)$ and $v_i(k)$ are the velocities of the particle $i$ at the next and current iterations respectively, $r_1(k)$ and $r_2(k)$ are random numbers between 0 and 1. $x_i(\mathrm{k})$ is the position of the particle at the current iteration , $p_{best,i}(\mathrm{k})$ is the personal best position of the particle, $g_{best}(\mathrm{k})$ is the global best position for the entire swarm. $c_1$ and $c_2$ are the acceleration coefficients known as the cognitive and the social coefficients that are typically chosen $\epsilon$ (1,2).

The inertia weight w controls the influence of the inertia component of the velocity. This parameter is used to keep the velocity from fast changes and decrease the exploration behavior of the swarm. It is found from the following equation [21]:

$$w = w_{max} - (w_{max} - w_{min})\frac{iter}{iter_{max}} \tag{5}$$

where $w_{max}$ , $w_{min}$ $are$ the maximum and minimum inertia weights respectively; $iter$ is the current iteration number and $iter_{max}$ is the maximum number of iterations.

After the velocities have been calculated, the positions of the particles are updated by the following equation:

$$x_i(k+1) = x_i(\mathrm{k}) + v_i(\mathrm{k}+1) \tag{6}$$

Then, the new positions are assigned with a new fitness value and the algorithm is repeated until the termination criterion is attained. The population size mostly used in PSO is $\epsilon$ (20,60); while $w$ is chosen less than 1 [20,22]. The properties chosen for the PSO in this paper are shown in the following table:

Table 2. PSO Parameters Properties

| Population size | 50 |
|---|---|
| Social acceleration coefficient ($C_2$) | 1.5 |
| Cognitive acceleration coefficient ($C_1$) | 1.5 |
| Maximum inertia weight ($w_{max}$) | 0.9 |
| Minimum inertia weight ($w_{min}$) | 0.4 |
| Maximum iteration number | 300 |

The maximum number of iterations was found to be high enough for the algorithm to converge to a solution. The speed response is required to have an optimal overall performance, which is minimum overshoot ($M_p$), rising time ($T_r$), settling time ($T_s$) and steady state error ($e_{ss}$). These requirements can be achieved by minimizing the error between the reference speed and the actual speed by using a specified criteria such as the integral of absolute error (IAE), the integral of time absolute error (ITAE) and the integral of time squared error (ITSE). The fitness function to be minimized chosen here is by using the IAE criteria; because the signal to be optimized is subjected to a disturbance (load) and this criteria treats all the error signal equally and thus, the effect of the disturbance is handled during the optimization process. The fitness value is obtained by running a simulation to the system with a predefined properties and calculating the sum of absolute error at the end of simulation. For each particle, the speed controller's parameters ($K_p$, $K_i$ and $K_d$) are set before the simulation with the particle's position and the simulation is run to obtain the corresponding fitness value of the particle. The best fitness value obtained is equal to 4.3469e6 by the following parameters: $K_p$ =0.39935, $K_i$ =0.17764 and $K_d$ =2.1372e-5.

The following flowchart shows the procedure of PSO method for the system:

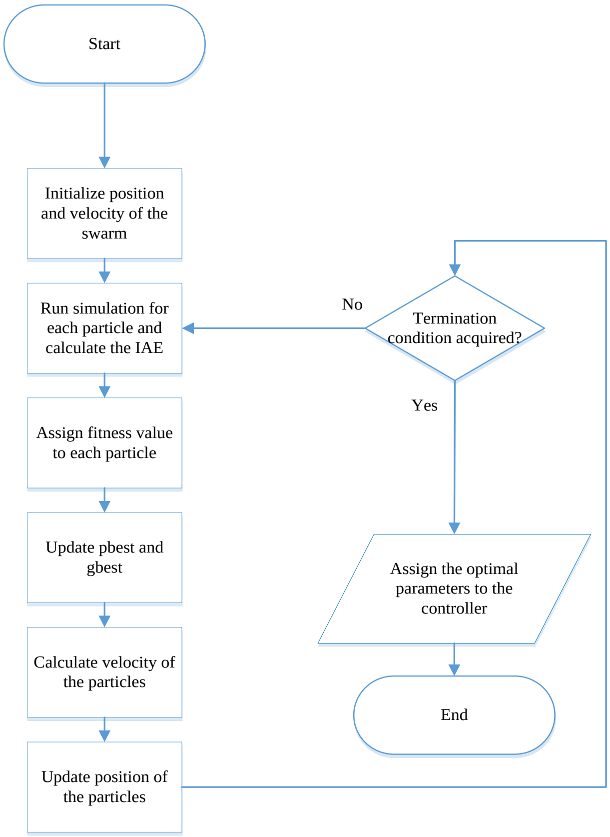


Figure 1. PSO Procedure Flowchart for the System.

## 6. Proposed System

The block diagram of the proposed system is show in the following figure:

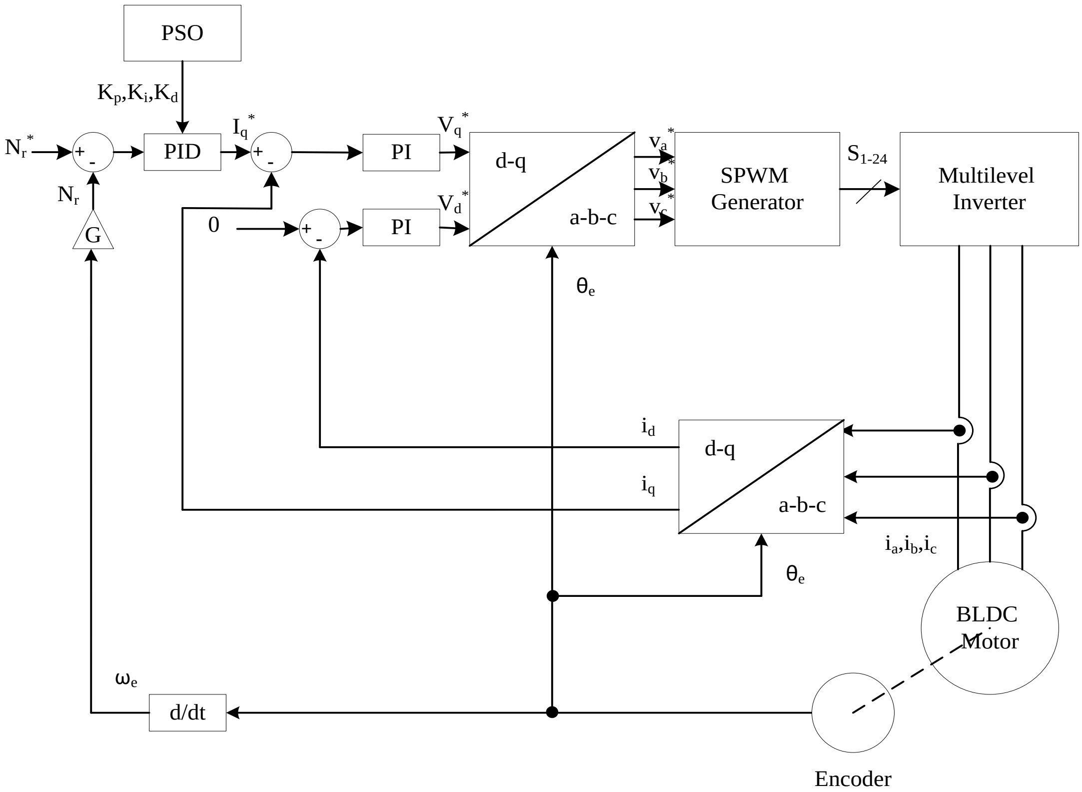


Figure 2. Overall System Block Diagram

The system consists of a BLDC motor that is fed from a five-level CHB inverter. The phase currents are transformed using Park transformation to the rotating reference frame. The position used in the Park-transformation is taken from an absolute position encoder, which is then differentiated to give the speed in rad/sec. The speed is then multiplied by a gain to convert it to rpm, which is compared with the reference speed to give the speed error. The speed error is then processed by the optimally tuned PID with PSO to give the reference torque component (reference quadrature current). The reference quadrature current is compared with the actual quadrature current and the error is processed by a PI controller to give the reference quadrature voltage. The reference direct current is set to zero since the flux is supplied by the permanent magnet; it is compared with the actual direct current and the error is processed by a PI controller to give the reference direct voltage. The direct and quadrature voltages are transformed to three-phase voltages using Park inverse transformation where the rotor position is also used. The three-phase voltages represent the modulating signals that are given to the SPWM generator, which outputs the gates signals of the inverter.

The closed-loop transfer function of the system is constructed based on the rotating reference frame (d-q axis). The voltage equations for the BLDC motor in the d-q axis are similar to the PMSM, which are given by [23]:

$$V_d = I_d R_s + L_s \frac{dI_d}{dt} - \omega_e L_s I_q \quad (7)$$

$$V_q = I_q R_s + L_s \frac{dI_q}{dt} + \omega_e \psi_d \tag{8}$$

where $V_d$, $V_q$, $I_d$ and $I_q$ are the voltages and currents in the d-q axis, $\omega_e$ is the electrical rotor speed and $\psi_d$ is d-axis flux-linkage.

Since vector control is applied to the motor, the two axis are controlled separately with the d-axis current set to zero by the PI controller. The transfer function for the two axis are:

$$\frac{I_d(s)}{V_d(s)} = \frac{I_q(s)}{V_q(s)} = \frac{\frac{1}{L_s}\frac{1}{s}}{1 + \frac{R_s}{sL_s}} = \frac{1}{sL_s + R_s} = \frac{\frac{1}{R_s}}{s\frac{L_s}{R_s} + 1} = \frac{K_c}{sT_c + 1} \tag{9}$$

where $K_c = \frac{1}{R_s}$ and $T_c = \frac{L_s}{R_s}$ , which is the electrical time constant of the motor. By adding the PI controllers, the transfer function becomes:

$$\frac{I_d(s)}{{I_d}^*(s)} = \frac{I_q(s)}{{I_q}^*(s)} = \frac{(\frac{sK_p + K_i}{s})(\frac{K_c}{1 + sT_c})}{1 + (\frac{sK_p + K_i}{s})(\frac{K_c}{1 + sT_c})} = \frac{sK_pK_c + K_iK_c}{s^2T_c + s\left(1 + K_pK_c\right) + K_iK_c} \tag{10}$$

where ${I_d}^*$and ${I_q}^*$ are the reference currents in d-q axis, $K_p$ and $K_i$ are the parameters of the PI controller.

The current control loop is then added to the mechanical equation of the motor (3) to obtain the overall transfer function as seen in the following figure:

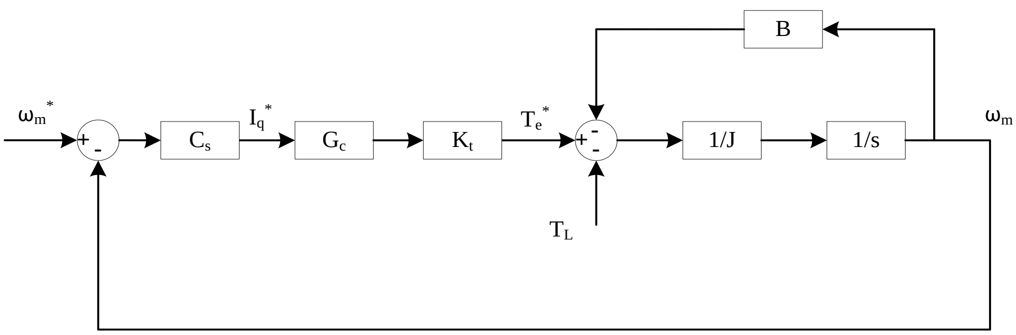


Figure 3. Simplified Overall System Block Diagram

where $C_s$ is the transfer function of the speed controller ($\frac{s^2K_d+sK_p+K_i}{s}$), $G_c$ is the transfer function of the current control loop, $\omega_m^*$ is the reference mechanical speed and $T_e^*$ is the reference electromagnetic torque. With $T_L$ is set to zero, the overall transfer function becomes:

$$\frac{\omega_m(s)}{{\omega_m}^*(s)} = \frac{C_sG_cK_t}{sJ + B} \tag{11}$$

## 7. Simulation Results and Discussion

The first simulation is done for the six-step or trapezoidal technique system; the speed controller for this system is a PI controller tuned with trial and error method. The reference is set at 3000 rpm at starting; then it is changed to 1500 at 0.5 sec; and then changed to 500 rpm at 0.7 sec. At time 0.1 s, a load torque of 3 N.m is added to the motor. The following figure shows the obtained speed response for the trapezoidal technique:

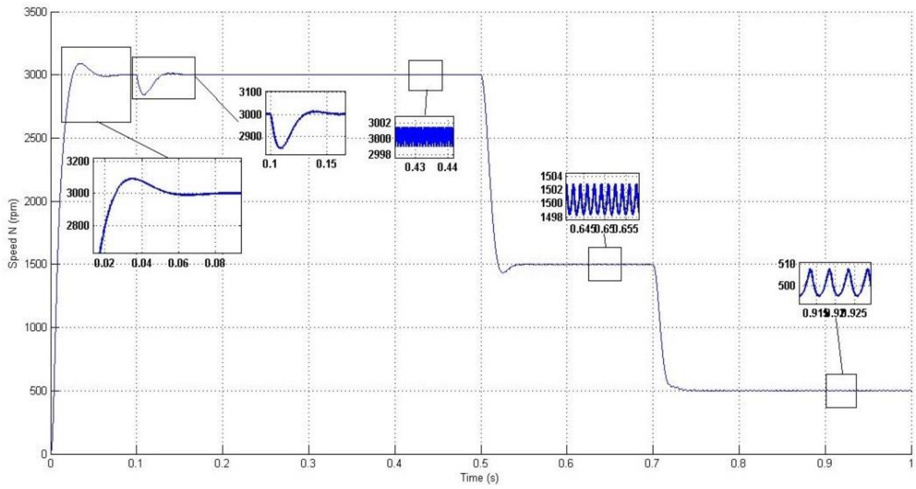


Figure 4. Speed Response of the Trapezoidal Technique

As observed from Fig. 4, the speed response has a $T_r$ of 0.0257 s, a $T_s$ of 0.08 s, an $M_p$ of 3% and an $e_{ss}$ of approximately zero. When the rated torque of  is applied to the motor, the speed drops to 2845 rpm and returns to the reference speed after a time of 0.016 s. The peak-peak speed ripple at rated torque is seen to be 0.08% at rated speed, 0.296% at 1500 rpm and 2.5% at 500 rpm. The waveforms of the stator current of phase a, BEMF of phase a and the electromagnetic torque of the trapezoidal technique are shown in the following figure:

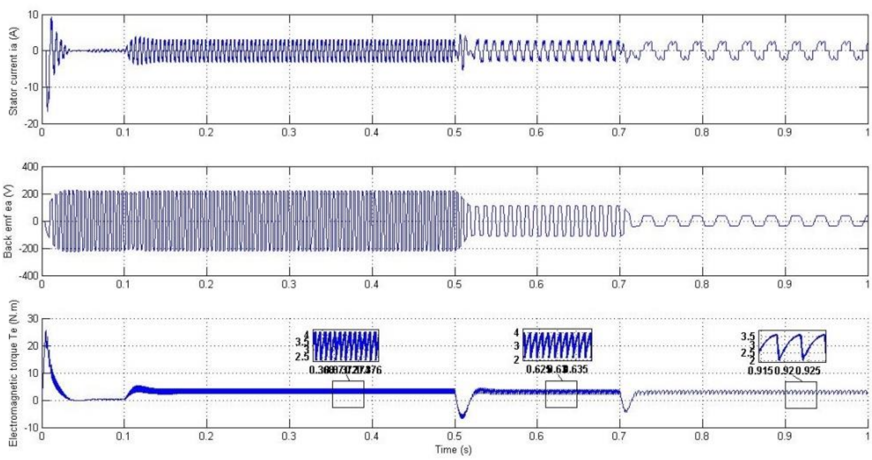


Figure 5. Stator Current, BEMF and Electromagnetic Torque Waveforms of the Trapezoidal Technique

The current waveform is seen from Fig. 5 to have a high distortion that is caused by the current commutation in the phases. The distortion in the currents causes the torque to have a high ripple, which is found from the waveform to be 57% at rated speed.

The second simulation is done for the proposed system in which the reference speed is set with same settings as the previous simulation. The speed controller is set with the optimal parameters obtained by PSO method. The obtained speed response is shown in the following figure:

From Fig. 6, it is seen that the speed response has a $T_r$ of 0.0142 sec, a $T_s$ of 0.05 sec, an $M_p$ of 0% and an $e_{ss}$ of 0.233%. The speed drops to 2993.5 rpm when the rated torque is applied at 0.1 s and returns to the reference speed after a time of 0.0018 s. The speed ripple at rated torque is 0.011% at 3000 rpm, 0.04% at 1500 rpm and 0.158% at 500 rpm. The following figure shows the waveforms of the stator current of phase a, BEMF of phase a and the electromagnetic torque of the proposed system:

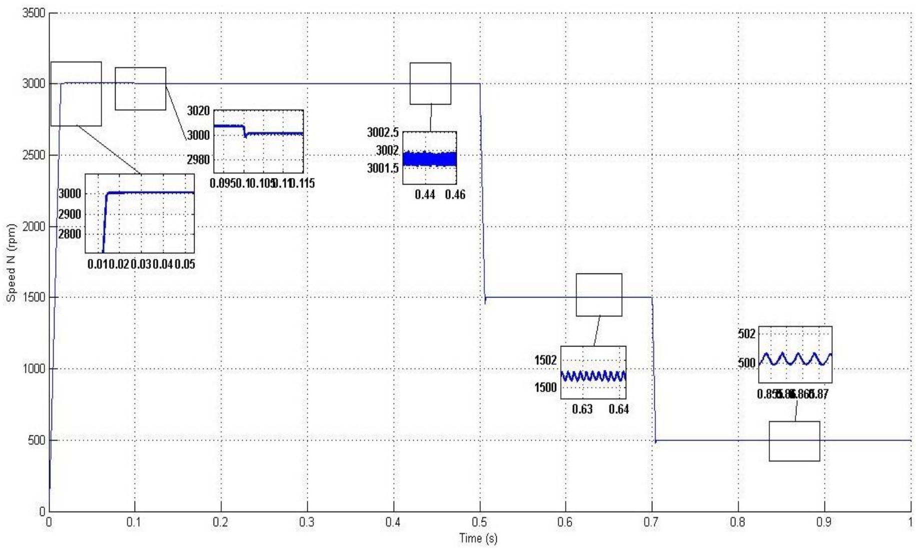


Figure 6. Speed Response of the Proposed System

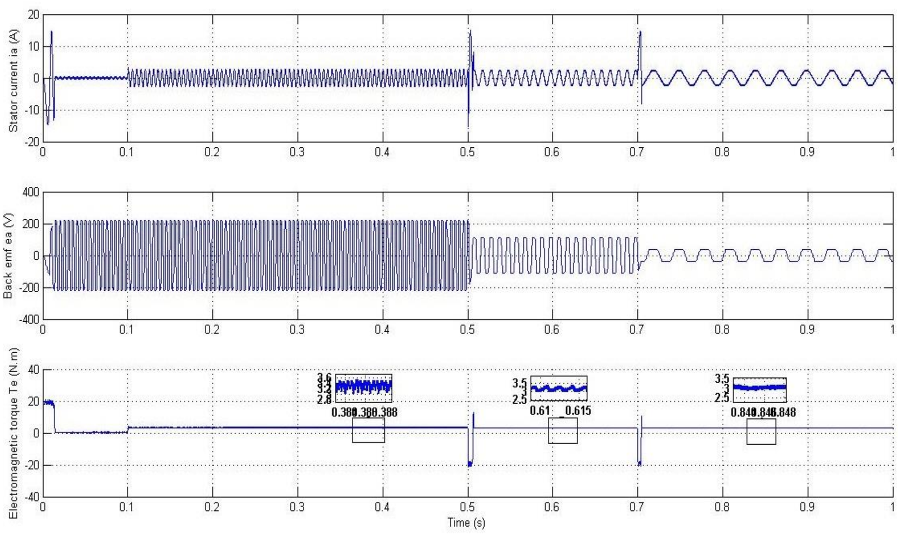


Figure 7. Stator Current, BEMF and Electromagnetic Torque Waveforms of the Proposed System

The current waveform as seen from Fig. 7 is very close to a sinusoidal shape with very little distortion. The current waveform became near sinusoidal due to the use of vector control; this causes the distortion due to the current commutation to be lessened. The staircase voltages generated by the multilevel inverter further reduces the distortion in the current waveform. Thus, the torque ripple is seen to be significantly reduced compared with the trapezoidal technique with it being 16% at rated speed.

The following table shows the THD results of the stator current and line-line voltage for the trapezoidal technique and the proposed system where it is seen that the THD is greatly lowered:

Table 3. THD Results

| Method | THD for the Line-Line Voltage (%) | THD for the Stator Current (%) |
|---|---|---|
| Trapezoidal Technique | 32.78 | 34.19 |
| Proposed System | 19.04 | 4.72 |

## 8. Conclusions and Future Work

In this paper, a BLDC motor drive system is proposed that achieves optimal speed response by using PSO method to find the optimal PID controller parameters; and achieves minimized torque ripple by using vector control to drive the motor with near sinusoidal currents. To further reduce the torque ripple, multilevel inverter is used to lower the THD of the voltages and current. The system is simulated in MATLAB/Simulink and the results is compared with the traditional trapezoidal method. The results show that the speed response is seen to improve greatly compared with the trapezoidal technique having a better overall performance; and the torque ripple and THD of the voltages and currents are significantly reduced.

A possible future work is to implement the system in practice using a microcontroller or Field Programmable Gate Array (FPGA).

## 9. References


1. C. Nilsson and D. Modrack, 2013, *"Universal Embedded Motor Control"*, Master's Thesis, Chalmers University of Technology, Sweden.
2. D. K. Kim , K. W. Lee,T. D. Kim and J. Y. Choi, 2004, *"Commutation Torque Ripple Reduction in a Position Sensorless Brushless dc Motor Drive"*, IEEE Trans. Power Electronics, vol. 21, no. 6, pp. 1762-1768, Germany.
3. S. Wang, 2008/2009, *"BLDC Ripple Torque Reduction via Modified Sinusoidal PWM"*, Fairchild Semiconductor Power Seminar, pp. 1-10.
4. M.A. Doss, E.Premkumar, G.R. Kumar and J. Hussain, Feb. 2013, *"Harmonics and Torque Ripple Reduction of Brushless DC Motor (BLDCM) using Cascaded H-Bridge Multilevel Inverter"*, IEEE International Conference on Power, Energy and Control (ICPEC), pp. 296-299, Dindigul.

5. K. Ang, G. Chong and Y. Li, July 2005, "*PID Control System Analysis, Design, and Technology"*, IEEE Transactions on Control Systems Technology, vol. 13, no. 4, pp. 559-576.
6. G. R. Yu and R. C. Hwang, Oct. 2004, *"Optimal PID Speed Control of Brushless DC Motors Using LQR Approach"*, IEEE International Conference on Systems, Man and Cybernetics, vol. 1, pp. 473 - 478.
7. A. Rubaai, M. J. C. Sitiriche and A. R. Ofoli, July/Aug. 2008, *"Design and Implementation of Parallel Fuzzy PID Controller for High-Performance Brushless Motor Drives: An Integrated Environment for Rapid Control Prototyping"*, IEEE Transactions on Industry Applications, vol. 44, no. 4,pp. 1090 – 1098.
8. R. Kandiban and R. Arulmozhiyal, Jan. 2012, *"Speed Control of BLDC Motor Using Adaptive Fuzzy PID Controller"*, Procedia Engineering International Conference on Modelling Optimization and Computing, vol. 38, pp. 306-313.
9. S. Ravi, D. N. Rao, K. M. Krishna and V. Mezhuyev, 2014, *"A Proposed GA Based PID Controller for Three Phase Brushless DC Motor"*, Universal Journal of Control and Automation (UJCA), vol. 2, no. 4 ,pp. 69-76.
10. S. Rathika and C. S. Ravichandran, Dec. 2014, *"PSO Based PID Controller for BLDC Motor"*, International Journal of Innovative Research in Science, Engineering and Technology (IJIRSET), vol. 3, no. 12.
11. S. W. Colton, June 2010, "*Design and Prototyping Methods for Brushless Motors and Motor Control"*, M.Sc. Thesis, Massachusetts Institute of Technology.
12. S. Rambabu, 2007, *"Modelling and Control of a Brushless DC Motor"*, M.Tech. Thesis, National Institute of Technology, Rourkela.
13. Y. I. Al Mashhadany, 2015, *"High-Performance Multilevel Inverter Drive of Brushless DC Motor"*, International Journal of Sustainable and Green Energy, Special Issue: Engineering Solution for High Performance of Solar Energy System. Vol. 4, No. 3-1, pp. 1-7.
14. D. M. Reed, Aug. 2009, *"Direct Field-Oriented Control of an Induction Machine Using an Adaptive Rotor Resistance Estimator"*, M.Sc. Thesis, The Pennsylvania State University.
15. *"Park, Inverse Park and Clarke, Inverse Clarke Transformations MSS Software Implementation"*, Microsemi User's Guide.
16. S. Khomfoi and L. M. Tolbert, 2007, *"Multilevel Power Converters"* Elsevier, in Power Electronics Handbook, pp. 451-482.
17. M. Derakhshanfar, 2010, *"Analysis of Different Topologies of Multilevel Inverters"*, M.Sc. Thesis, Chalmers University of Technology, Sweden.
18. V. Naumanen, 2010, *"Multilevel Converter Modulation: Implementation and Analysis"*, Sc.D Thesis, University of Technology, Lappeenranta.
19. S. Devarakonda, May 2012, *"Particle Swarm Optimization"*, M.Sc. Thesis, University of Dayton, Ohio.
20. G. I. Evers, May 2009, *"An Automatic Regrouping Mechanism to Deal with Stagnation in Particle Swarm Optimization"*, M.Sc. Thesis, University of Texas-Pan American, Edinburg, T.

21. A. Mahor, V. Prasad and S. Rangnekar, Oct. 2009, *"Scheduling of Cascaded Hydro Power System: A New Self Adaptive Inertia Weight Particle Swarm Optimization Approach"*, IEEE International Conference on Advances in Recen Technologies in Communication and Computing (ARTCOM).
22. S. Talukder, Feb. 2011, *"Mathematical Modelling and Applications of Particle Swarm Optimization"*, M.Sc. Thesis, Blekinge Institute of Technology, Sweden.
23. M. Peter, M. Pavol and V. Ján, 2010, *"PI-Controllers Determination for Vector Control Motion"*, Proceedings of the Annual Conference Tehnical Computing, vol. 18, pp. 70-77.